

Received April 1, 2019, accepted April 26, 2019, date of publication May 1, 2019, date of current version May 14, 2019.

Digital Object Identifier 10.1109/ACCESS.2019.2914259

The Algorithm of Concrete Surface Crack Detection Based on the Genetic Programming and Percolation Model

ZHONG QU^{1,2}, YU-XIANG CHEN¹, LING LIU³, YI XIE¹, AND QIANG ZHOU²

¹School of Software Engineering, Chongqing University of Posts and Telecommunications, Chongqing 400065, China

²College of Computer Science and Technology, Chongqing University of Posts and Telecommunications, Chongqing 400065, China

³College of Mobile Telecommunications, Chongqing University of Posts and Telecommunications, Chongqing 401520, China

Corresponding author: Zhong Qu (quzhong@cqupt.edu.cn)

This work was supported in part by the Chongqing Basic and Frontier Research Project under Grant cstc2015jcyjBX0090, and in part by the Scientific and Technological Research Program of Chongqing Municipal Education Commission under Grant KJ1600434.

ABSTRACT Because of the impact of the variation in different concrete surface images, such as the heterogeneity of the detection environment, uneven illumination, stains, the block, and water leakage, the existing crack detection algorithms cannot detect the real crack quickly and effectively. In this paper, a genetic algorithm based on genetic programming (GP) and percolation model is proposed. This method involves three steps. First, the cracks are pre-extracted by the image processing model of GP. Second, the crack tip is calculated after the crack skeleton is extracted. With the endpoint as the anchor point, high speed, and high precision percolation are used to detect the cracks with small width accurately. Concurrently, the fracture unit areas are scanned for connection. Finally, the pre-extracted cracks are connected with the cracks detected by the percolation, and the mass interference area is removed to obtain the real cracks on the concrete surface. The simulation results show that the concrete surface crack detection algorithm based on the GP and percolation model can effectively combine both of their advantages. The algorithm proposed in this paper can detect real concrete surface cracks accurately and effectively with strong robustness.

INDEX TERMS Concrete surface crack detection, genetic programming, percolation model, skeleton extraction.

I. INTRODUCTION

Concrete surface cracks are the main form of structural problems for buildings, bridges, tunnels, roads, and other infrastructure. A vicious cycle easily forms through the interaction of cracks and natural hazards, which reduces the safety, stability, and reliability of infrastructure. At worst the situation, the safety of people is endangered. To evaluate the stability of infrastructures after structural damage, and to grasp the crack morphology and pathological degree of the cracking, it is necessary to detect the concrete surface cracks. The result of detection can also provide a basis for the safety assessment and damage management of infrastructures.

Researchers have proposed a variety of crack detection methods based on digital image processing. In 2000, Lee et al. [1] presented a simple and easy nondestructive evaluation procedure for identifying a crack, the location and

size of the crack. In 2010, Yamaguchi and Hashimoto [2]–[4] proposed a crack detection algorithm based on the percolation model and proposed the termination and jump conditions to improve the detection speed. The algorithm has high accuracy, but it has a profusion of redundant computations. In 2016, Qu et al. [5], [6] proposed an improved crack detection algorithm based on percolation model. This method improves the percolate conditions and pre-extracted seed pixel based on sliding window. The percolation calculation of the background noise pixels is reduced, and the accuracy of crack detection is improved after percolating and crack connecting two times. In 2015, Yun et al. [7], [8] proposed a flexible pavement crack identification and segmentation algorithm based on morphological processing. The MorphLink-C algorithm, which detects cracks mainly based on morphological processing, may cause distorted results.

With the development of machine learning, its technology has also been applied to pavement inspection.

The associate editor coordinating the review of this manuscript and approving it for publication was Dong Wang.

In 2008, Vakil-Baghmisheh *et al.* [9] presented a fault diagnosis method based on genetic algorithms (GAs) and a model of damaged (cracked) structure. Zhen *et al.* [10] presented a novel and effective approach to automatic 3D Facial Expression Recognition (FER), based on the Muscular Movement Model (MMM). The muscular areas by using a Genetic Algorithm (GA) was proposed in the learning step. Nakayama and Nagao [11], Nishikawa *et al.* [12] proposed a genetic programming (GP) model based on the crack detection algorithm with tree structure training used for image filtering. It has the advantages of automatic detection and high efficiency, but it also has some shortcomings, such as partial fracture and less detection accuracy for the cracks with small width. Existing methods [13]–[15] can perform well on saliency object detection in MSRA-1000 dataset. In 2016 Shi *et al.* [16] proposed crack forest, a novel road crack detection framework based on random structured forests, to detect cracks. The detection rate of this algorithm has a good performance. In 2016, Amhaz *et al.* [17], [18] presented an algorithm for crack detection based on the selection of minimal paths, in a fully unsupervised manner. In 2012 and 2016, Zou *et al.* [19], [20] proposed an automatic crack detection algorithm and a pavement shadow removal revisited (PSRR) algorithm respectively. The PSRR builds a crack probability map using the tensor voting, derives a minimal spanning tree from this map, and conducts a recursive tree-edge pruning to identify desirable cracks. The algorithm can effectively remove the shadows.

In 2018, Chen *et al.* [21] proposes a deep learning framework, based on a convolutional neural network (CNN) and a Naïve Bayes data fusion scheme. In 2017, Cha *et al.* [22] proposed a vision-based method using a deep architecture of convolutional neural networks (CNNs) for detecting concrete cracks without calculating the defect features. This algorithm can detect the areas where the cracks are located but it can't extract cracks. In 2016, Zhang *et al.* [23] proposed a depth convolutional neural network algorithm to detect road cracks. The accuracy and recall rate is more than 85%, but there is a certain degree of error on the edge of cracks. In 2016, Yoo and Kim [24] proposed an artificial neural network and logistic regression analysis technology to realize the automatic detection of cracks, but these two algorithms cannot solve the problem of detection accuracy for cracks of small width.

In this paper, a new algorithm is proposed for concrete surface crack detection algorithm based on the GP and percolation model in three steps. Firstly, the cracks are pre-extracted by the crack detection model of GP, which is utilized to train the best crack detection model. Multiple concrete surface images of different crack characteristics are selected as the training set to get this model. Then the thin cracks are detected by the percolation algorithm based on the results of the previous test. Finally, the error detection area is removed by calculating the roundness and the length characteristics of the connected region in the detection results. Thus, the final test result is obtained.

II. IMAGE PROCESSING MODEL BASED ON THE GENETIC ALGORITHM

A. GP ALGORITHM

Based on Darwin's theory of evolution, evolutionary algorithms solve the problem of self-organization and adaptive artificial intelligence technology through the simulation of biological evolution process and mechanism. Evolutionary algorithms include genetic algorithms, GP, evolutionary programming and evolution strategy. The frameworks of GP algorithm and simple genetic algorithm have the same description. But, there are differences in the modes of evolution, especially in tree structures and gene structures. The basic principle of GP algorithm is selection and change. It differs from other search methods in two salient features: first, the algorithm is based on populations; secondly, there is competition among individuals in the population. In order to search for a specific query, a tool is needed that intelligently generates a set of queries and evaluates whether they can export the same set of objects as given by the user.

The GP theory is applied to the concrete crack detection. By integrating the existing image edge detection algorithm and image filter, such as mean filter and Gaussian filter, a tree crack detection model is constructed. The model is trained by the acquired image set. Thus, the detection model is obtained. Then, this model is used to detect the cracks on the concrete surface. The detection model structure is shown in Figure 1. F_1 , F_2 , F_3 are image processing operations which include some image filters and edge detection operators. I represents the input image, and O is the output result.

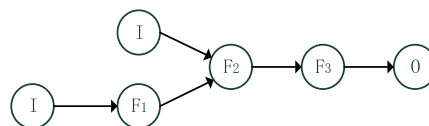


FIGURE 1. Crack detection model.

B. DESIGN OF THE IMAGE PROCESSING MODEL BASED ON THE GENETIC ALGORITHM

During image processing, the model of GP algorithm can use the existing filter based on the tree structure model to train the optimal model of image processing [25]. As shown in Figure 2, the source image is the original image, the objective image is the result of the processing, and the unknown image processing model is obtained by the GP algorithm.

C. EXPERIMENTAL IMAGE SET

The accuracy of image segmentation depends on the resolution and image contrast. The concrete surface image has the characteristics of a complex background, uneven illumination, and stains, whilst the shape of the cracks is complex. These conditions can have a certain influence on the detection results. Accordingly, it is necessary to select the images with different shape features to verify the reliability of the algorithm.

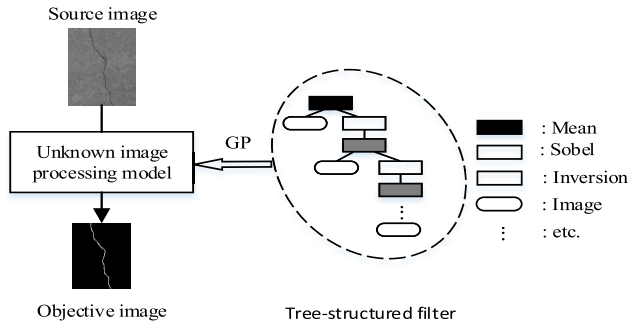


FIGURE 2. Schematic diagram of the image processing model.

In this paper, several actual images were taken as the experimental image set, as shown in Figure 3. Data sets with more than 500 concrete surface images of size 3200×2400 were taken by a regular Nikon camera with back-illuminated complementary metal-oxide semiconductor (CMOS) and 14 times optical zoom. To compare the performance of different algorithms, original images were down-sampled in this paper. The algorithm used for image ‘down-sampling’ is image Pyramid. Down-sampling is not necessary in practical applications. After the down-sampling, the different background images with crack were sized to 400×300 [pixel], as shown in Figure 3. Our experimental environment is: intel Core(TM) i7-7700 CPU @ 3.60GHz. Due to the color information on concrete surface, the 8 bits depth gray image set was utilized to improve the efficiency of the algorithm.

In order to verify the performance of the algorithm, the results in this paper were compared with the manually extracted reference. The artificial extraction result image was obtained by the following steps: First, the crack location was plotted on the original images manually by professional persons with engineering technology, and the pixel value of the crack was set to 0. Then the artificial extractions were obtained by converting down images into binary ones. The original images are down-sample image as shown in Figure 3 (1)-(4) and Figure 3 (9)-(12). The artificial images are shown in Figure 3 (5)-(8) and Figure 3 (13)-(16).

According to the image acquisition time and the crack characteristics, 20 training images were obtained by stratified sampling in the image set, as shown in Figure 4. Figure 4 (1)-(5) are the original images of the experiment, Figure 4 (6)-(10) are the artificial extractions as the target images in this paper. Figure 4 (11)-(15) are the weighted images, obtained by inverting the target image color and set the background pixel value as $1/2V_{ax}(V_{ax} = 255)$.

D. NODE FUNCTION

The tree structure is used to organize the genes in the GP algorithm. The branch node is the processing function, the leaf node is the input image, and the root node is the output result. In the concrete surface images, the cracks are linear and multi branch. Moreover, the uneven illumination, stain marks, falling blocks, and water leakage will result in low image

contrasts and further impact on the detection. In order to improve the accuracy of the image processing, Sobel operator and Laplacian algorithm are used as the main edge detection function.

In the paper by Aoki and Nagao [26], a known image’s filters are used as the node processing function. In every single input function, $F = \{f_{ij}\}$ is the input image, $G = \{g_{ij}\}$ is the output image. For each double input function, the input image can be represented by $F_1 = \{f_{1ij}\}$ and $F_2 = \{f_{2ij}\}$. In addition, the pixel values of the image are represented in an integer between 0 and V_{max} . If g_{ij} is less than 0, the pixel value is set to be 0. If g_{ij} is greater than V , the pixel value is set to be V_{max} .

E. EVALUATION FUNCTION

In the process of training the prediction model, individual evaluation function [23] is defined as follows (1),

$$E \equiv \frac{1}{N} \sum_{k=1}^N \left[R_k \frac{\sum_{i=1}^{w_k} \sum_{j=1}^{h_k} W_k(i, j) \cdot |O_k(i, j) - T_k(i, j)|}{\sum_{i=1}^{w_k} \sum_{j=1}^{h_k} W_k(i, j) \cdot V_{max}} \right] \quad (1)$$

where k is the number of images; O_k , T_k and W_k are the k -th original, target, and weight image respectively, $R_k \equiv \left[\frac{w_k \cdot h_k}{\bar{w} \cdot \bar{h}} \right]^{1/2}$, and V_{max} is the pixel with maximum value equaled to 255. w_k and h_k are the width and length of the image, respectively.

F. IMPROVED SELECTION OPERATOR

To restrain the expansion of the training model, the previous cross operation [14] uses the roulette wheel selection crossover operator to select the second trees’ hybrid nodes, as shown in equation (2),

$$p = \frac{1}{\theta^{n-X} \cdot N_s} \quad (2)$$

where p is the selection ratio of second crossing node, θ is a random constant, n is the first hybrid node of the sub-tree size, X is the selected node sub-tree size, and N_s is the number of X tree nodes.

Although the roulette wheel operator can effectively restrain the expansion of the training model, there is a problem of slow convergence speed. It takes more than 20 days to train the 20000 generation on a personal computer. In order to shorten the time needed for training, a double tournament that applies two layers of tournaments in a series (first for fitness and then for parsimony) is used in this paper. The idea of the algorithm is as follows:

- i. If the principle of evaluation priority (or the principle of node size priority) is chosen, then the node size is considered;
- ii. The parameter M ($M = 1-2$) of the operator is used to control the selection probability. Take the evaluation or node size as the probability of selecting operator dependence to $M/2$. When $M = 1$, random selection of evaluation or

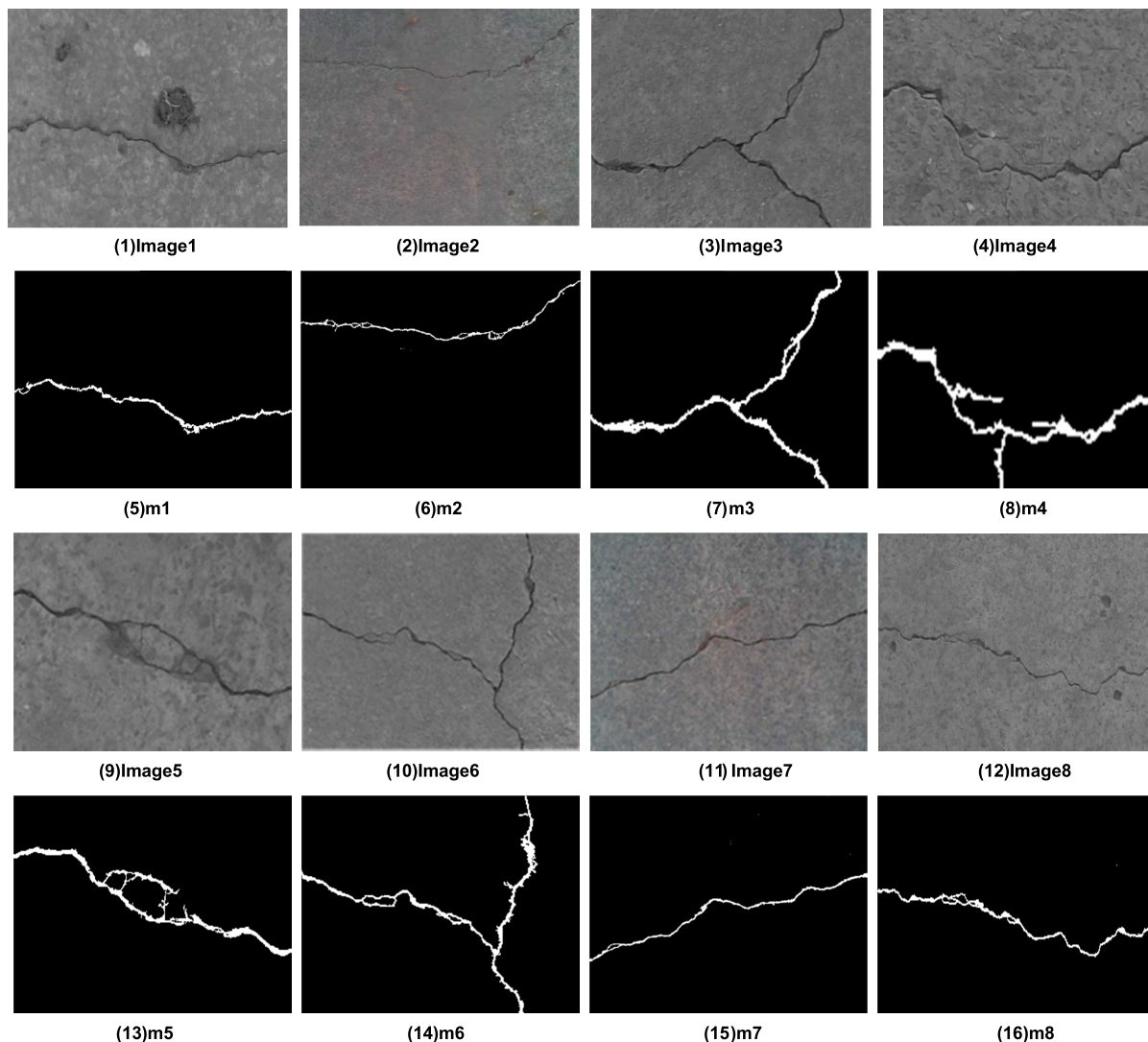


FIGURE 3. The original images are down-sample image as shown in (1)-(4) and (9)-(12). The artificial images are shown in (5)-(8) and (13)-(16).

node size is chosen as operator dependency; when $M = 2$, select both evaluation and node size as the selection operator dependency.

G. TRAINING THE GP MODEL

The idea of the detection algorithm based on the GP is as follows:

- i. Randomly generate 500 tree models with a depth of 2-5, as mentioned in Figure 1 and Figure 2. In the training image, the root node is the target image, the branch node is the node function, and the leaf node is the original image.
- ii. The evaluation of each spanning tree model is calculated by Equation (1), and then the parents of the next generation of individuals (Tree Image Processing Model) are selected based on a double tournament operator.
- iii. Two pairs of parents are screened out in ii and then cross-mutate them to generate the next generation of individuals.

- iv. Repeat iii to generate 500 individuals and calculate evaluation for each individual.

- v. Repeat steps ii-iv until the evaluation level meets the requirement, then get the final image processing model as shown as Figure 2.

The training course of the image processing model is shown in Figure 5.

In this paper, the double tournament operator is used as the GP selection operator, and the training time can be reduced to 3 hours. The evaluation of the GP algorithm in the 200 generation is no longer convergent. At this point the evaluation of the algorithm has also reached the appropriate value. The evaluation of the training process is shown in Figure 6.

III. PERCOLATION MODE

Percolation is a variable local processing method. It takes full account of the connectivity of gray values between neighboring pixels. This algorithm can ensure the continuity of the crack with the gray and shape features used to detect the

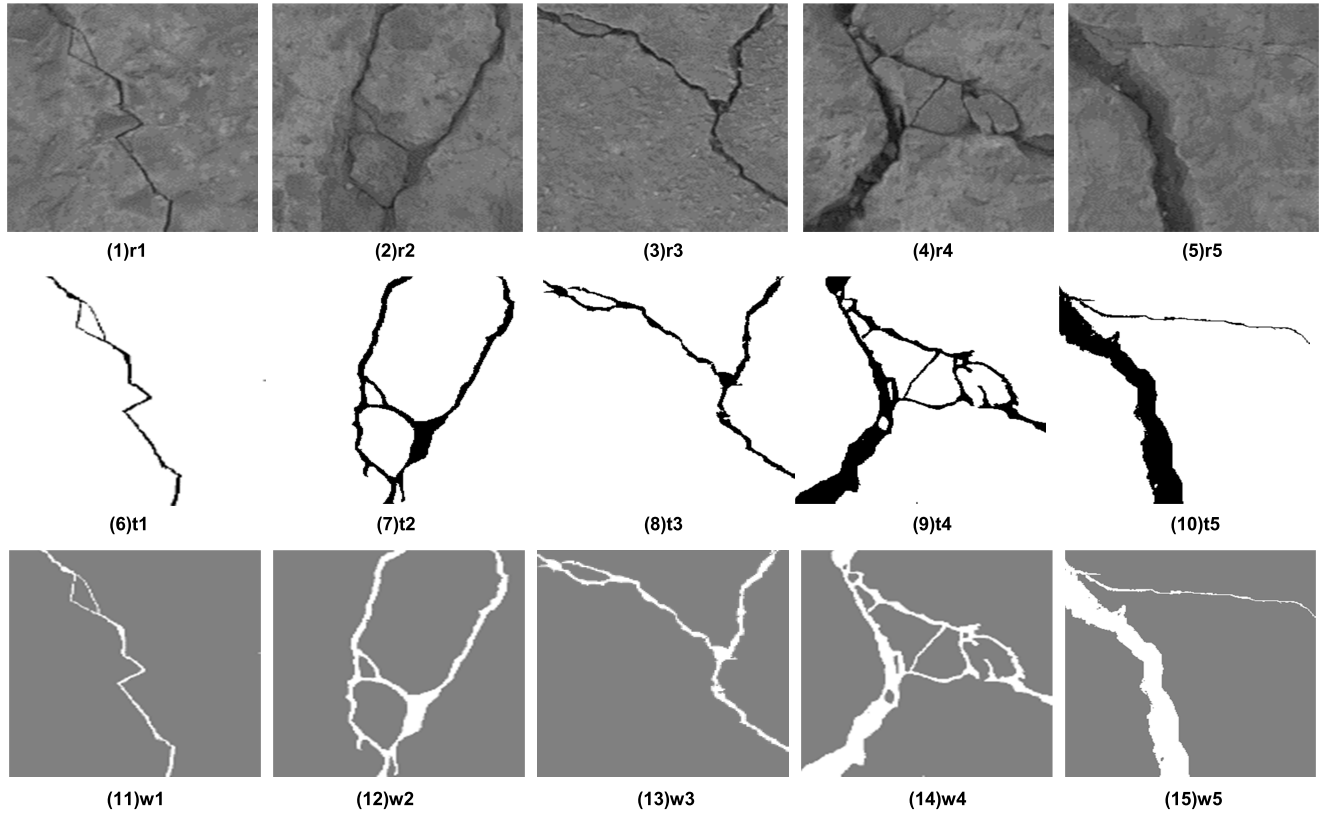


FIGURE 4. (1)r1-(5)r5 are the original images of the experiment, (6)t1-(10)t5 are the artificial extractions as the target images in this paper, (11)w1-(15)w5 are the weighted image.

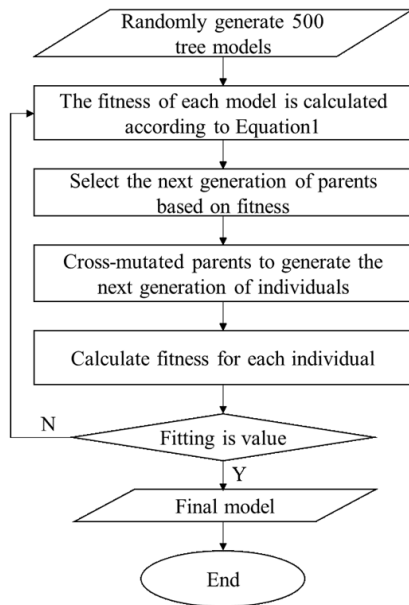


FIGURE 5. Flow chart of the GP.

cracks. The basic idea is to start at an initial pixel, and then extend to the surrounding area according to the probability of P which is easy to measure, then the maximum value of P in the nearest neighborhood can be percolated. By repeating

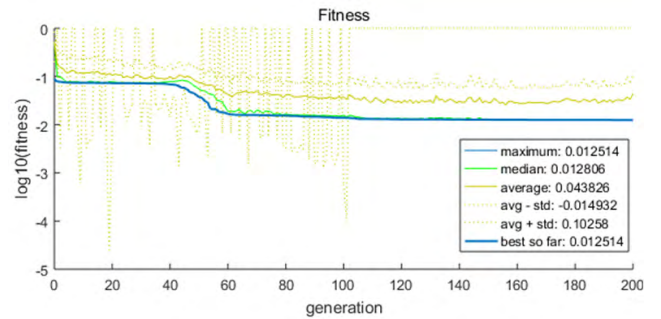


FIGURE 6. Evaluation of the GP.

the percolated treatment, the area will be extended until it reaches the boundary [27], [28].

In order to evaluate whether the percolate zone is a legitimate crack area, the circularity of the percolated area is needed in the process of percolation. Circularity is shown in equation (3),

$$F_c = 4 \times C_{count} / (\pi \times C_{max}^2) \quad (3)$$

where C_{count} is the number of pixels of the percolation zone Dp , and C_{max} is the minimum diameter of the circumscribed circle of Dp . The range of F_c is from 0 to 1. If the center pixel belongs to the crack area, the percolated area will grow

linearly, with F_c close to 0. If the center pixel is the background pixel, the percolated area will grow in two-dimension, with F_c close to 1. Therefore, according to F_c , which is the characteristics of D_p , the center pixel P can be determined as a legitimate crack pixel.

The percolation model is used to deal with the experimental with Figure 7 (1)-(2). The results are shown in Figure 7 (3)-(4). The algorithm has a high accuracy of crack extraction.

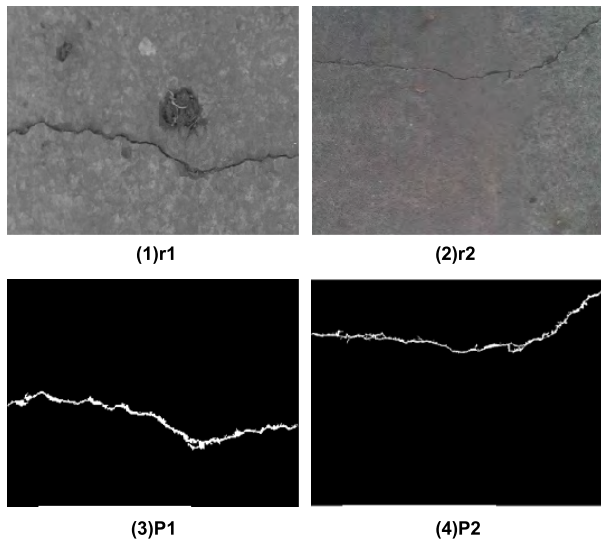


FIGURE 7. Results of the Percolation model.

A. DE-NOISING ALGORITHM

Because of the characteristics of the crack and the background noise, the gray features and shape features can be considered. Based on the percolation model, if F_c of the pixel p satisfies $I(p) < F_cMax \times 255$, remove the noise. F_cMax is the max of F_c , in a percolate zone and it is the upper limit. The main idea of the de-noising algorithm [4] is as follows:

- i. The p_c of the central pixel, which is needed to be de-noised, is added to the pixel set D_p .
- ii. The 8 neighborhoods of each pixel in the D_p constitute a candidate region D_c . For any pixel $p_c \in D_c$, if $I(p_c) < F_cMax \times 255$, the p_c will be added to the D_p .
- iii. The radius of minimum circumscribed circle of D_p is calculated, and then F_c is calculated according to equation (3). If it satisfies the conditions in equation (4), D_p is the noise domain, and all pixels are determined as background pixels; otherwise, all pixels are determined as crack pixels.

$$F_c > F_cMax || radius < radiusMax \quad (4)$$

where $radiusMax$ is the threshold of maximum radius in de-noised cluster.

B. CONNECTION ALGORITHM BASED ON THE IMAGE SKELETON EXTRACTION

In some cases, the detection results of percolation may cause crack fracture in the detection process, and the de-noising on

the serious fractured detection results would be de-noised with a part of short cracks together. If the noises are not processed immediately, the results will be mixed with a large number of noises. A connection algorithm [13] based on the crack skeleton is as follows:

- i. The percolated treatment results are used to remove the noise of point and block, and the hole is filled by the dilation erosion operation;
- ii. Use 8 direction chain code and the Zhang *et al.* [23] parallel thinning algorithm for image thinning algorithm to refine the image to get a single pixel skeleton;
- iii. The connected region R_l of skeleton in the image is divided, and the number of pixels N_l for each connected region is calculated;
- iv. If $N_l > N_t$, it will be connected to the end of the skeleton in the region recorded as D_l . Set its state as UNUSED and add the endpoint to set P_{end} . N_t for the empirical value;
- v. Select a point D_l with UNUSED state in set P_{end} . From this point, the 5 adjacent pixels on the skeleton are scanned. Then these points are fitted by linear fitting, with the straight line is recorded as α_1 ;
- vi. According to the equation (5) along the direction of the straight line, in the range of a certain angle of the τ area to search for the conditional pixel D'_l to be connected,

$$\begin{cases} p \in R_l \&\& p' \notin R_l \\ d < d_{T_{min}} || \theta < \theta_T \\ d < d_{T_{max}} \end{cases} \quad (5)$$

where d is the connection distance between D_l and D'_l , $d_{T_{max}}$ is the largest connection distance threshold, and $d_{T_{min}}$ is the threshold when the angle of the minimum connection distance is ignored. The angle between the connecting line and straight line is calculated as $\theta = \arctan \left| \frac{\tan \alpha_2 - \tan \alpha_1}{1 + \tan \alpha_1 \tan \alpha_2} \right|$, θ_T is the angle threshold, where α_2 is a linear $D_l D'_l$ perspective. In this paper, empirical values are obtained, $d_{T_{max}} = 25$, $d_{T_{min}} = 15$, $\alpha_T = 20$;

vii. The width of the connecting line between the connecting crack and the connecting frame is calculated, and then the D_l and the D'_l are connected by a straight line on the original image and the skeleton image respectively. The connection region of the skeleton image is then updated and N_l is recalculated.

viii. Repeat step (iv)-(vii) until the point set P_{end} is emptied.

C. DETECTION ALGORITHM BASED ON THE GP AND PERCOLATION MODEL

GP algorithm has the advantages of high efficiency and low sensitivity to crack width, but it has a disadvantage of low precision for cracks with small width detection. The crack detection algorithm based on percolation model has the advantage of high precision of cracks with small width detection, but it has disadvantages of high computational

complexity and difficulty of parameter setting. To realize the accurate and fast detection of cracks, a new genetic algorithm based on the GP and percolation model is proposed in this paper. The core algorithm steps are described as follows:

- i. The improved GP algorithm is used to train the optimal image processing model, and the model is used to extract the original cracks and remove the noise.
- ii. The Zhang parallel thinning algorithm [29] is used to extract the skeleton of the target. With a single pixel being processed, the burr is eliminated by the optimized 8 direction chain code scanning and tracking principle. Then the calculation of the crack skeleton endpoints and construction of the endpoint set P_{end} are made.
- iii. Take a point as the anchor in P_{end} , the detection region of high efficiency and high accuracy percolated detection algorithm will be identified as the crack areas are added to the pre-image. Repeat the operation until the point set of all points in P_{end} are processed, and then the image of precise detection is achieved.
- iv. Extract the skeleton of the fine detection image and eliminate the burr. Then, the crack detection algorithm based on image segmentation is used to connect the cracks in the fine detection image.

The flow chart of genetic algorithm based on the GP and percolation model is shown in Figure 8.

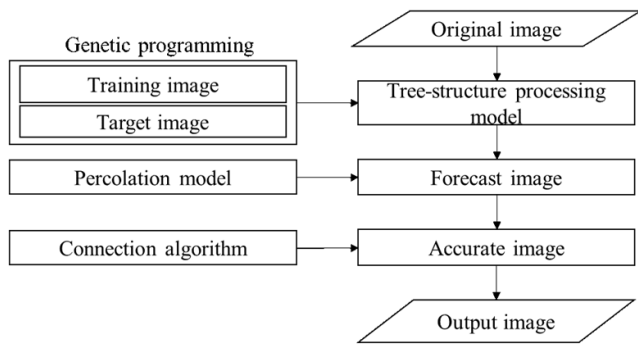


FIGURE 8. GP and flow model detection algorithm flow.

TABLE 2. Quantitative analysis of GP.

| Image | Percolation (%) | | | | | GP (%) | | | | | The proposed method(%) | | | | |
|-----------|-----------------|----------|-----------|----------------------|------------|----------|----------|-----------|----------------------|------------|------------------------|----------|-----------|----------------------|------------|
| | <i>P</i> | <i>R</i> | <i>NR</i> | <i>F_i</i> | <i>FPR</i> | <i>P</i> | <i>R</i> | <i>NR</i> | <i>F_i</i> | <i>FPR</i> | <i>P</i> | <i>R</i> | <i>NR</i> | <i>F_i</i> | <i>FPR</i> |
| Fig.3 (1) | 74.29 | 65.87 | 25.71 | 69.83 | 0.380 | 68.42 | 65.78 | 31.58 | 67.07 | 0.046 | 99.72 | 95.31 | 0.280 | 97.47 | 0.004 |
| Fig.3 (2) | 92.18 | 77.91 | 7.82 | 84.45 | 0.074 | 78.45 | 66.16 | 21.55 | 71.78 | 0.200 | 99.05 | 94.62 | 0.950 | 96.78 | 0.009 |
| Fig.3 (3) | 99.87 | 81.76 | 0.83 | 89.96 | 0.016 | 84.37 | 84.22 | 15.63 | 84.30 | 0.620 | 99.91 | 97.62 | 0.040 | 98.80 | 0.002 |
| Fig.3 (4) | 91.81 | 82.61 | 8.19 | 86.97 | 0.410 | 76.04 | 63.73 | 23.96 | 69.34 | 1.190 | 91.96 | 80.41 | 8.040 | 85.80 | 0.400 |
| Fig.3 (5) | 19.80 | 18.35 | 80.20 | 19.05 | 2.520 | 75.24 | 78.14 | 24.76 | 76.66 | 0.780 | 99.62 | 96.76 | 0.380 | 98.17 | 0.011 |
| Fig.3 (6) | 99.07 | 81.91 | 9.30 | 89.68 | 0.029 | 65.64 | 90.34 | 34.36 | 76.03 | 1.060 | 98.72 | 98.32 | 1.280 | 98.52 | 0.039 |
| Fig.3 (7) | 97.07 | 84.76 | 2.93 | 90.50 | 0.031 | 79.49 | 75.20 | 20.91 | 77.29 | 0.220 | 99.75 | 98.40 | 0.250 | 99.07 | 0.003 |
| Fig.3 (8) | 99.05 | 75.39 | 9.5 | 85.62 | 0.016 | 86.53 | 68.20 | 13.47 | 76.28 | 0.230 | 99.56 | 99.20 | 0.440 | 99.38 | 0.007 |

TABLE 1. Confusion matrix.

| Real Image | Detection Result | | |
|------------|------------------|----------|-------|
| | Positive | Negative | Total |
| Positive | TP=True | FP=False | TP+FP |
| Negative | FN=False | TN=True | FP+TN |
| Total | TP+FP | FP+TN | |

IV. ANALYSIS OF EXPERIMENTAL RESULTS

A. ALGORITHM PERFORMANCE EVALUATION

Image crack detection is a typically binary classification problem. According to the combination of the real category and the prediction model of the processing model, the sample can be divided into four types, which are the true positives (TP), the false positives (FP), the true negatives (TN) and the false negatives (FN).

Corresponding to the number of samples, the performance verification of the algorithm uses the confusion matrix classification of accuracy evaluation method [25] to show the quantitative analysis experiment in this paper. The confusion matrix of the classification results is shown in Table 1.

The Precision, Recall, True Positives Rate, False Positives Rate and Noise Rate are defined below as the comprehensive evaluation indexes:

$$P = \frac{TP}{TP + FP}, \quad R = \frac{TP}{TP + FN}, \quad NR = \frac{FP}{TP + FP},$$

$$FPR = \frac{FP}{FP + TN}, \quad F_1 = \frac{2PR}{P + R}$$

where TP represents the number of crack pixels that are classified correctly in the test results; $TP + FN$ and $FP + TN$ represents the number of crack pixels and background pixels in real artificially extracted image respectively; $TP + FN$ is the number of crack pixels detected and FP is the number of crack pixels that are detected as background pixels.

B. ALGORITHM PERFORMANCE ANALYSIS

This paper proposes a crack detection algorithm based on the genetic algorithm and the percolation model of the

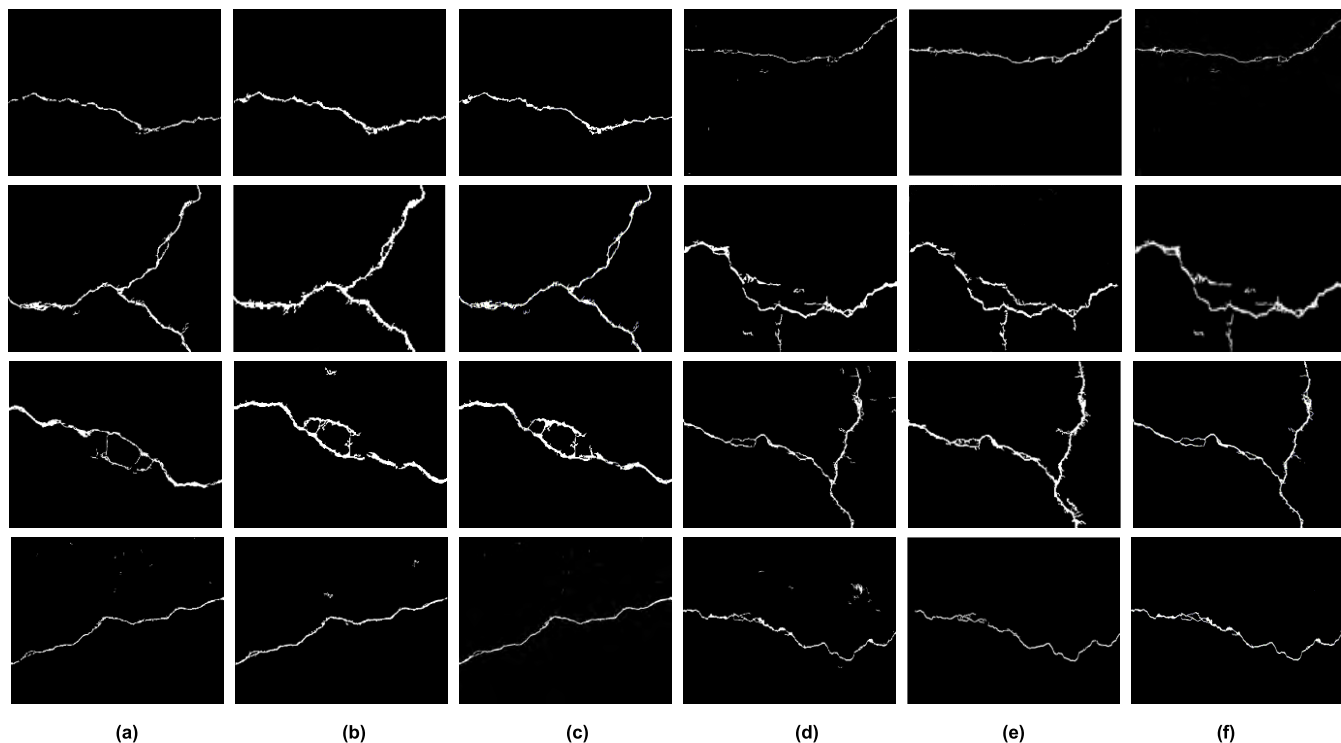


FIGURE 9. Experimental results of different algorithms. (a) GP. (b) Percolation. (c) The proposed method. (d) GP. (e) Percolation. (f) The proposed method.

crack detection algorithm to process the experimental results and verify the performance of the algorithm (shown in Figure 9).

The image processing model obtained by the algorithm in Section 2.3 is used to process the experimental data in Figure 3, with the results are shown in Figure 9 (a) and (d).

The percolation model in Section 2.4 is used to process the experimental data in Figure 3, with the results are shown in Figure 9 (b) and (e).

Based on the genetic algorithm and the percolation model, four experiments are carried out to process the experimental data in Figure 3, and ground true data sets are the target images. The results are shown in Figure 9(c) and (f).

As shown in Table 2, the detection accuracy for the trained image detection model of the GP algorithm is high. Most of the images have better effects, but the accuracy of the high noise and cracks in fuzzy edge is lower, resulting in less robustness of the algorithm. The detected results have fracture.

The accuracy of overall detection in the percolation model is relatively stable and it has strong robustness. The crack fracture is less, and the detection is better than the algorithm without considering the crack edge information which has poor detected edge results with some burr.

These three algorithms previously mentioned and the results of artificial extraction (Figure 3) are analyzed quantitatively. The proposed algorithm can make up for the shortcomings of the fracture. The algorithm can better detect the edge of the crack with robustness.

TABLE 3. Algorithm run time comparison.

| Image | GP | Percolation model | The proposed method |
|---------------|--------|-------------------|---------------------|
| Fig. 10 (a)1 | 0.181s | 1.698s | 0.283s |
| Fig. 10 (a) 2 | 0.173s | 1.747s | 0.351s |
| Fig. 10 (a)3 | 0.182s | 1.454s | 0.242s |
| Fig. 10 (a)4 | 0.177s | 1.402s | 0.220s |
| Fig. 10 (a)5 | 0.179s | 0.566 | 0.211s |
| Fig. 10 (a)6 | 0.175s | 0.736s | 0.224s |
| Fig. 10 (a)7 | 0.180s | 0.815s | 0.357s |
| Fig. 10 (a)8 | 0.183s | 0.882s | 0.375s |

Figure 10 is the experimental results of different illuminations.

In Figure 10, each column is a group of images. The first and second rows are natural environment obtained with lack of illumination. All the algorithm results show satisfied precision. The third and fourth rows are night obtained with fill flash, together with the Random Structured Forest (RSF) [16]. The results have more fractures. The fifth and sixth rows are night obtained with no illumination. With RSF, it is difficult to detect complete cracks and all algorithms have unsatisfactory detection results of minuteness crack. The seventh and eighth rows are images of inhomogeneous illumination, based on night and daytime respectively. The

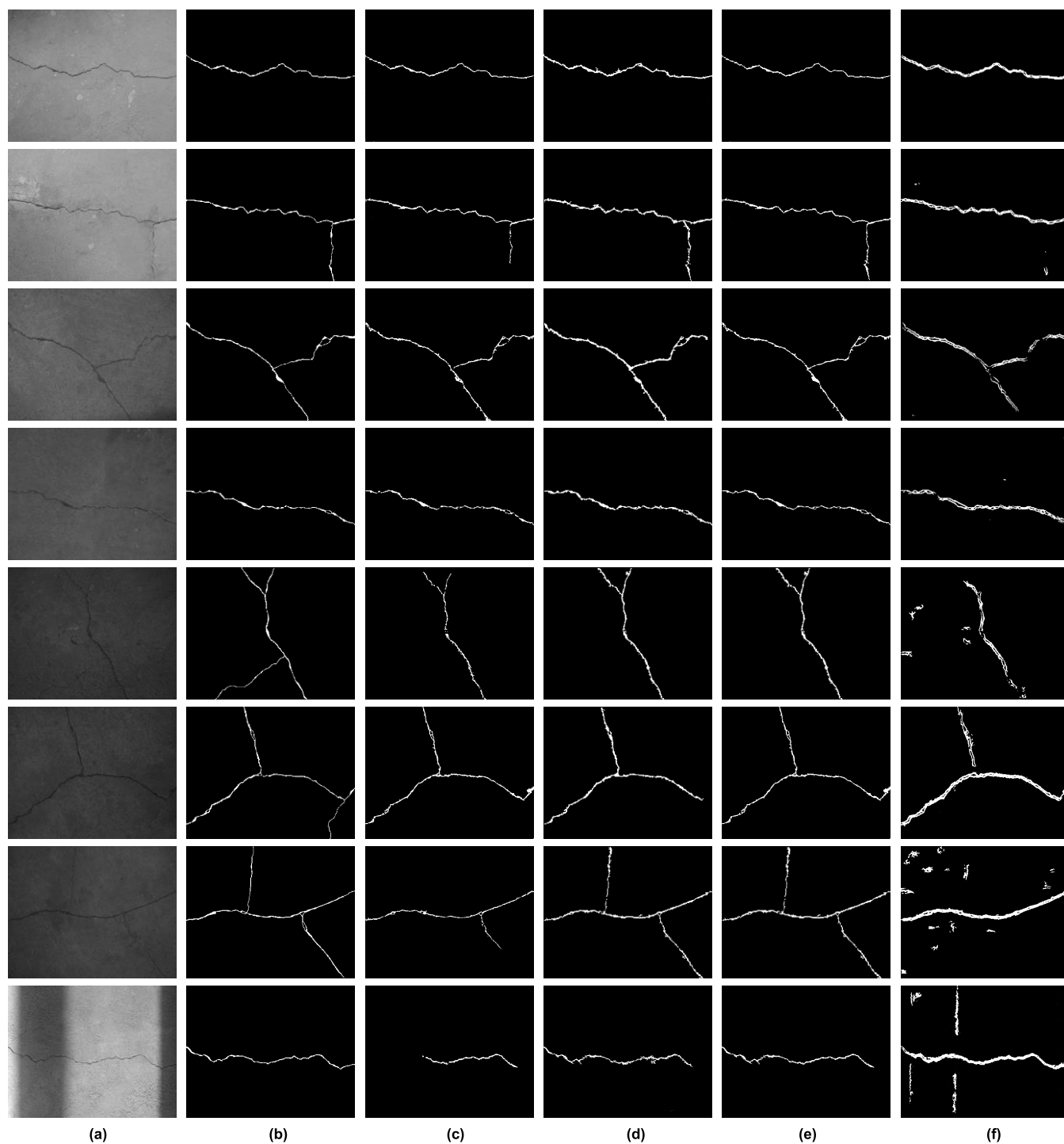


FIGURE 10. Each column is a group of images. The first and second rows are natural environment obtained with lack of illumination. The third and fourth rows are night obtained with fill flash. The fifth and sixth rows are night obtained with no illumination. The seventh and eighth rows are images of inhomogeneous illumination, based on night and daytime respectively. (a) Original Image. (b) Artificial extraction. (c) GP. (d) Percolation. (e) The proposed method. (f) RSF.

other algorithms have hiatus in varying degrees. To sum up, the proposed algorithm manifests good precision in homogeneous illumination with other algorithms, regardless of daytime or nighttime. Although there is a partial hiatus under inhomogeneous illumination, the proposed algorithm still

maintains high effectiveness compared with other algorithms. Illumination is still the linchpin and aporia in the field of crack detection.

Table 3 shows the time required for the three algorithms to process different images. According to the data in the table,

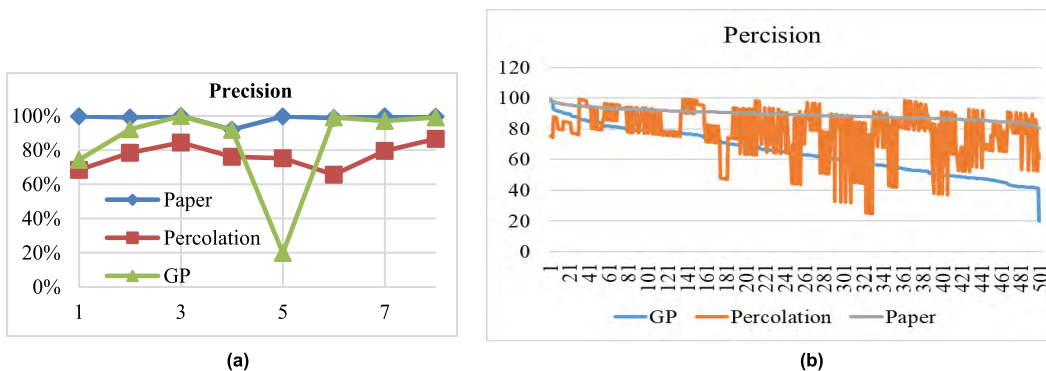


FIGURE 11. Precision (include 8 images and 500 images in our laboratory’s data set). (a) 8 images. (b) 500 images.

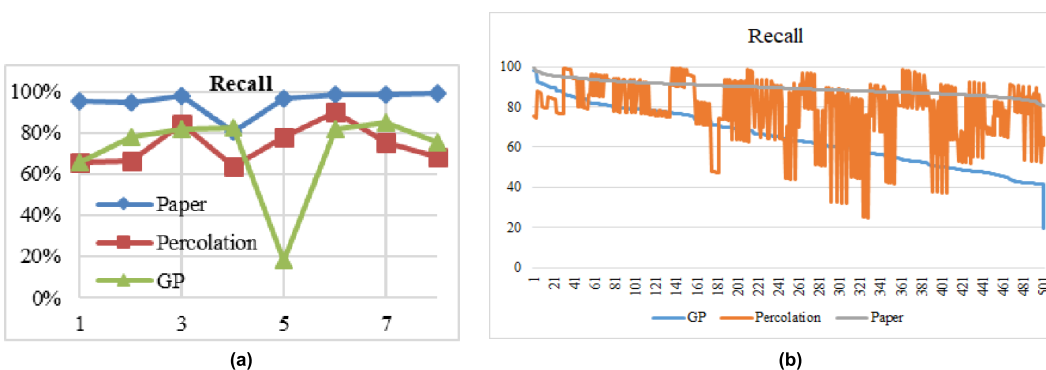


FIGURE 12. Recall (include 8 images and 500 images in our laboratory’s data set). (a) 8 images. (b) 500 images.

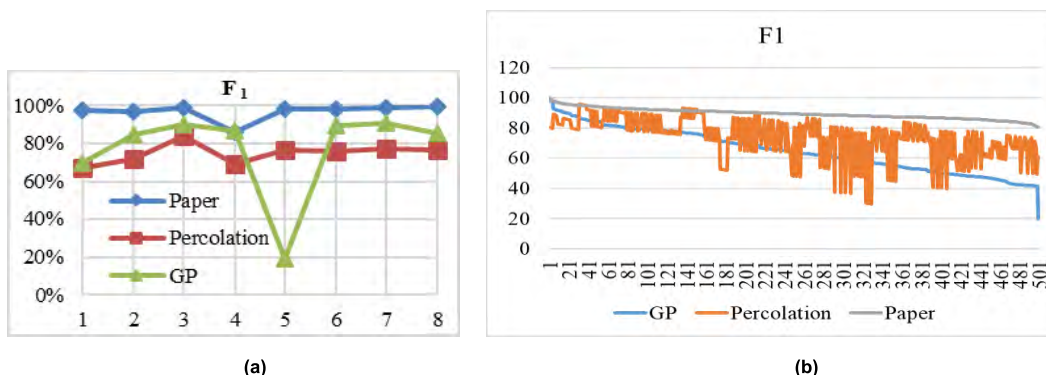


FIGURE 13. F1 (include 8 images and 500 images in our laboratory’s data set). (a) 8 images. (b) 500 images.

the GP algorithm has the advantages of high efficiency but low precision. The Percolation algorithm has high precision, but the processing time is related to the length of the crack in the image. Our proposed algorithm presents high efficiency to a certain extent based on the consideration advantages of GP algorithm. At the same time, due to the double-layer competition selection operator, our algorithm is faster than the original GP algorithm model on training time. Thus, there is a significant improvement in the accuracy of detection result.

Figure 11, 12 and 13 describe the recall rate, precision rate and F1 of these three algorithms respectively (include 8 images and 500 images in our laboratory’s data set). It is

obvious that the algorithm proposed in this paper has a higher precision and recall rate compared with the other two algorithms. At the same time, the algorithm also has strong robustness.

V. CONCLUSION

In this paper, the proposed algorithm takes full account of the specific characteristics of the concrete surface. Firstly, it reduces the training time of the genetic algorithm by improving the selection operator, with the original image extracted by using the optimal training model. Secondly, the Zhang parallel skeleton extraction algorithm is used to extract the skeleton of the pre-extracted crack. Then, the crack

terminal node is calculated. Thirdly, the terminal node is used as the anchor point, which is combined with the percolation detection algorithm to detect the cracks with small width accurately. Finally, the fracture crack is connected by the region extension algorithm, and the accurate crack image is obtained by de-noising.

The experimental results show that the algorithm not only can quickly and accurately detect the concrete surface cracks, but also can effectively eliminate the interference factors, such as the stain, the block, water leakage, etc. In order to improve the detection accuracy, the internal function of the improved tree model can be considered in future research. Furthermore, further investigation into the problem of slow convergence speed is recommended in future studies.

ACKNOWLEDGMENT

The authors wish to thank the editors and anonymous reviewers for their valuable comments and suggestions on this paper.

REFERENCES

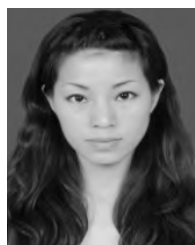
- [1] Y.-S. Lee and M.-J. Chung, "A study on crack detection using eigenfrequency test data," *Comput. Struct.*, vol. 77, no. 3, pp. 327–342, 2000.
- [2] T. Yamaguchi and S. Hashimoto, "Image processing based on percolation model," *IEICE Trans. Inf. Syst.*, vol. 89, no. 7, pp. 2044–2052, 2006.
- [3] T. Yamaguchi and S. Hashimoto, "Fast crack detection method for large-size concrete surface images using percolation-based image processing," *Mach. Vis. Appl.*, vol. 21, no. 5, pp. 797–809, 2010.
- [4] T. Yamaguchi, S. Nakamura, R. Saegusa, and S. Hashimoto, "Image-based crack detection for real concrete surfaces," *IEEJ Trans. Elect. Electron. Eng.*, vol. 3, no. 1, pp. 128–135, 2008.
- [5] Z. Qu, L.-D. Lin, Y. Guo, and N. Wang, "An improved algorithm for image crack detection based on percolation model," *IEEJ Trans. Elect. Electron. Eng.*, vol. 10, no. 2, pp. 214–221, 2015.
- [6] Z. Qu, Y. Guo, F. R. Ju, L. Liu, and L.-D. Lin, "The algorithm of accelerated cracks detection and extracting skeleton by direction chain code in concrete surface image," *Imag. Sci. J.*, vol. 64, no. 3, pp. 119–130, 2016.
- [7] H. B. Yun, S. Mokhtari, and L. Wu, "Crack recognition and segmentation using morphological image-processing techniques for flexible pavements," *Transp. Res. Rec.*, vol. 2523, pp. 115–124, 2015.
- [8] L. Wu, S. Mokhtari, A. Nazef, and B. H. Nam, "Improvement of crack detection accuracy using novel crack de-fragmentation technique in image-based road assessment," *J. Comput. Civil Eng.*, vol. 30, no. 1, pp. 1–17, 2015.
- [9] M.-T. Vakil-Baghmisheh, M. Peimani, M. H. Sadeghi, and M. M. Etefagh, "Crack detection in beam-like structures using genetic algorithms," *Appl. Soft Comput.*, vol. 8, no. 2, pp. 1150–1160, 2008.
- [10] Q. Zhen, D. Huang, Y. Wang, and L. Chen, "Muscular movement model-based automatic 3D/4D facial expression recognition," *IEEE Trans. Multimedia*, vol. 18, no. 7, pp. 1438–1450, Jul. 2016.
- [11] K. Nakayama and T. Nagao, "Automatic construction of image transformations to produce variously stylized painterly images," in *Proc. Eur. Modeling Symp.*, Nov. 2013, pp. 243–248.
- [12] T. Nishikawa, J. Yoshida, T. Sugiyama, and Y. Fujino, "Concrete crack detection by multiple sequential image filtering," *Comput. Aided Civil Infrastruct. Eng.*, vol. 27, no. 1, pp. 29–47, 2012.
- [13] Z. Wang, D. Xiang, S. Hou, and F. Wu, "Background-driven salient object detection," *IEEE Trans. Multimedia*, vol. 19, no. 4, pp. 750–762, Apr. 2017.
- [14] J. Lei et al., "A universal framework for salient object detection," *IEEE Trans. Multimedia*, vol. 18, no. 9, pp. 1783–1795, Sep. 2016.
- [15] F. Meng, H. Li, G. Liu, and K. N. Ngan, "Object co-segmentation based on shortest path algorithm and saliency model," *IEEE Trans. Multimedia*, vol. 14, no. 5, pp. 1429–1441, Oct. 2012.
- [16] Y. Shi, L. Cui, Z. Qi, F. Meng, and Z. Chen, "Automatic road crack detection using random structured forests," *IEEE Trans. Intell. Transp. Syst.*, vol. 17, no. 12, pp. 3434–3445, Dec. 2016.
- [17] R. Amhaz, S. Chambon, J. Idier, and V. Baltazart, "A new minimal path selection algorithm for automatic crack detection on pavement images," in *Proc. ICIP*, Oct. 2014, pp. 788–792.
- [18] R. Amhaz, S. Chambon, J. Idier, and V. Baltazart, "Automatic crack detection on two-dimensional pavement images: An algorithm based on minimal path selection," *IEEE Trans. Intell. Transp. Syst.*, vol. 17, no. 10, pp. 2718–2729, Oct. 2016.
- [19] Q. Zou, Z. Hu, L. Chen, Q. Wang, and Q. Li, "Geodesic-based pavement shadow removal revisited," in *Proc. (ICASSP)*, Mar. 2016, pp. 1761–1765.
- [20] Q. Zou, Y. Cao, Q. Li, Q. Mao, and S. Wang, "CrackTree: Automatic crack detection from pavement images," *Pattern Recognit. Lett.*, vol. 33, no. 3, pp. 227–238, 2012.
- [21] F.-C. Chen and M. R. Jahanshahi, "NB-CNN: Deep learning-based crack detection using convolutional neural network and naïve bayes data fusion," *IEEE Trans. Ind. Electron.*, vol. 65, no. 5, pp. 4392–4400, May 2018.
- [22] Y.-J. Cha, W. Choi, and O. Büyükoztürk, "Deep learning-based crack damage detection using convolutional neural networks," *Comput. Aided Civil Infrastruct. Eng.*, vol. 32, no. 5, pp. 361–378, 2017.
- [23] L. Zhang, F. Yang, Y. D. Zhang, and Y. J. Zhu, "Road crack detection using deep convolutional neural network," in *Proc. (ICIP)*, Sep. 2016, pp. 3708–3712.
- [24] H.-S. Yoo and Y.-S. Kim, "Development of a crack recognition algorithm from non-routed pavement images using artificial neural network and binary logistic regression," *KSCE J. Civil Eng.*, vol. 20, no. 4, pp. 1151–1162, 2016.
- [25] Z. Qu, L. Bai, S.-Q. An, F.-R. Ju, and L. Liu, "Lining seam elimination algorithm and surface crack detection in concrete tunnel lining," *J. Electron. Imag.*, vol. 25, no. 6, pp. 1–17, 2016.
- [26] S. Aoki and T. Nagao, "Automatic construction of tree-structural image transformation using genetic programming," in *Proc. Int. Conf. Image Process.*, Oct. 1999, pp. 529–533.
- [27] S. Luke and L. Panait, "A comparison of bloat control methods for genetic programming," *Proc. J. Evol. Comput.*, vol. 14, no. 3, pp. 309–344, 2006.
- [28] W. Waegeman, B. De Baets, and L. Boullart, "ROC analysis in ordinal regression learning," *Pattern Recognit. Lett.*, vol. 29, no. 1, pp. 1–9, 2008.
- [29] D. Zhang, Q. Li, Y. Chen, M. Cao, L. He, and B. Zhang, "An efficient and reliable coarse-to-fine approach for asphalt pavement crack detection," *Image Vis. Comput.*, vol. 57, pp. 130–146, Jun. 2017.



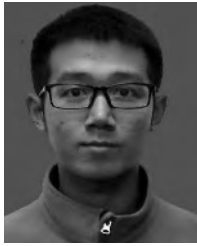
ZHONG QU received the M.S. degree in computer architecture the Ph.D. degree in computer application technology from Chongqing University, in 2003 and 2009, respectively. He is currently a Professor with the Chongqing University of Posts and Telecommunications. His research interests include digital image processing, digital media technology, and cloud computing.



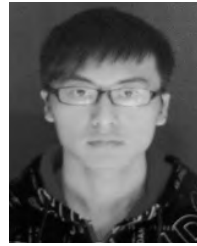
YU-XIANG CHEN received the M.S. degree in software engineering from the Chongqing University of Posts and Telecommunications, in 2018. His main research interest is digital image processing.



LING LIU received the M.S. degree in computer technology from the Chongqing University of Posts and Telecommunications, in 2014. Her main research interest is digital image processing.



YI XIE is currently pursuing the M.S. degree with the School of Software Engineering, Chongqing University of Posts and Telecommunications. His main research interest is digital image processing.



QIANG ZHOU is currently pursuing the Ph.D. degree with the School of Computer Technology Engineering, Chongqing University of Posts and Telecommunications. His main research interest is digital image processing.

...